Observations of non-solar-type dynamo processes in stars with shallow convective zones

S. V. Jeffers, J.-F. Donati, E. Alecian, S. C. Marsden

Monthly Notices
of the
ROYAL ASTRONOMICAL SOCIETY

Mon. Not. R. Astron. Soc. **411,** 1301–1312 (2011) doi:10.1111/j.1365-2966.2010.17762.x

Observations of non-solar-type dynamo processes in stars with shallow convective zones⋆

S. V. Jeffers,[1]† J.-F. Donati,[2] E. Alecian[3] and S. C. Marsden[4]

[1]*Sterrenkundig Instituut, Universiteit Utrecht, PO Box 80000, NL-3508 TA Utrecht, the Netherlands*
[2]*LATT, Observatoire Midi-Pyrénées, 14, avenue Edouard Belin, F-31400 Toulouse, France*
[3]*Observatoire de Paris, LESIA, 5, place Jules Janssen, F-92195 Meudon Principal Cedex, France*
[4]*Anglo Australian Observatory, PO Box 296, Epping, NSW 1710, Australia*

Accepted 2010 September 23. Received 2010 September 23; in original form 2010 February 13

ABSTRACT

The magnetic field topology and differential rotation are fundamental signatures of the dynamo processes that generate the magnetic activity observed in the Sun and solar-type stars. To investigate how these dynamo processes evolve in stars with shallow convective zones, we present high-resolution spectropolarimetric observations of the young GO dwarf HD 171488 over three epochs. Using the Zeeman–Doppler tomographic imaging technique, we have reconstructed surface brightness images that are dominated by polar and high-latitude starspots and a magnetic field topology that shows large-scale radial and azimuthal magnetic field components. Over the time-span of our observations, we do not observe a reversal of the magnetic field polarity as has been observed in other solar-type stars with shallow convective zones. The phase coverage of our data was sufficient to determine the differential rotation for two epochs where in conjunction with previous work, we conclude that there is no evidence for the temporal evolution of differential rotation.

Key words: stars: activity – stars: individual: HD 171488 – stars: magnetic field – stars: solar-type – starspots.

1 INTRODUCTION

The stellar dynamo manifests itself in the form of starspots, chromospheric plages and coronal emission. In the case of the Sun, the most prominent evidence of the magnetic field regeneration by dynamo processes is the reversal of the magnetic field every 11 yr. This process is considered to be generated by an $\alpha\Omega$ dynamo located in the tacoline at the base of the convection zone. However, for other solar-type stars, a detection of a full reversal of magnetic field has only been confirmed for the planet-hosting star τ Boo (Donati et al. 2008; Fares et al. 2009).

A crucial ingredient in the dynamo generation process is differential rotation, which is caused by the interaction of rotation and convection, leading to a redistribution of heat and angular momentum inside the convection zone. The investigation of the differential rotation, magnetic field topology and polarity of late-type stars allows the understanding of how the dynamo operates at different rotation rates, the importance of the tachocline and dependence on convection zone depth. Using Doppler imaging techniques, it has been shown by Barnes et al. (2005) that there is a steady increase in the magnitude of differential rotation towards earlier spectral types, i.e. with the shrinking of the star's convective zone. The differential rotation measurement of HD 171488, by Jeffers & Donati (2008) in Paper I, shows a result that is much higher than predicted by Barnes et al. (2005) for early G dwarfs (with $\mathrm{d}\Omega = 0.52 \pm 0.4$ rad d^{-1}). Similarly, high levels of differential rotation have also been measured on τ Boo (F7V) (Donati et al. 2008; Fares et al. 2009) where the latitudinal angular rotation $\mathrm{d}\Omega = 0.50 \pm 0.12$ rad d^{-1}. This is surprising given that HD 171488 is more active, due to its (i) shorter rotation period of 1.3 d, compared to 3–4 d for τ Boo, and (ii) different mass, 1.2 $\mathrm{M}_{\odot}$ compared to 1.42 $\mathrm{M}_{\odot}$ for τ Boo and hence fractional convective zone depth. The resulting convective turnover time for HD 171488 is therefore four times greater than that for τ Boo and a Rossby number that is an order of magnitude greater for τ Boo than for HD 171488. The results for HD 171488 and τ Boo are consistent with measurements of differential rotation of other late F stars (e.g. Reiners 2006).

The first long-term analysis of the temporal evolution of differential rotation has been determined for the K0V dwarf AB Dor (Donati, Collier Cameron & Petit 2003b; Jeffers, Donati & Collier Cameron 2007). The results, which span from 1992.05 to 2001.99,

⋆Spectropolarimetric observations were obtained, from 2007 May 21–26, 2007 November 8–13 and 2008 May 26–30 with the NARVAL echelle spectropolarimeter at the Telescope Bernard Lyot (Observatoire du Pic du Midi, France).

†E-mail: s.v.jeffers@uu.nl

show variations on a time-scale of at least 1 yr and show no evidence yet for any cyclic behaviour. AB Dor also does not show a magnetic field reversal over the time-span of the observations. Other stars with measurements of differential rotation spanning more than one epoch include LQ Hya (Donati et al. 2003b), R58 (Marsden et al. 2005) and IM Peg (Marsden et al. 2007).

Additionally, differential rotation has been measured using magnetic features, which have shown to give a measurement of differential rotation twice that of the brightness data for AB Dor (Donati et al. 2003b). This is interpreted as being evidence for a distributed dynamo operating throughout the convective zone and not confined to its base as in the solar dynamo. However, for HD 171488 in Paper I we measure a value of differential rotation using the magnetic features that is equivalent to that measured for the brightness data. This is consistent with the result from AB Dor as HD 171488 has a much thinner convective zone. Further evidence for a distributed dynamo in both AB Dor and HD 171488 is the presence of a large-scale toroidal field.

The motivation for this work is to use spectropolarimetric data to determine (1) the temporal evolution of the differential rotation on HD 171488, as has been measured on other late-type stars such as AB Dor, and (2) a change in the magnetic field polarity in case there is any, as has been observed on τ Boo. In this paper, we present new observations of HD 171488 obtained from 2007 May 21 to 26, 2007 November from 8 to 13 and 2008 May 26 to 30 with the spectropolarimeter NARVAL at the Telescope Bernard Lyot. We describe the data analysis and stellar parameter determination in Section 2. In Section 3 we present the surface brightness images and magnetic field topologies for each epoch, and in Section 4 we determine the differential rotation of HD 171488. We discuss the implications of our results in Section 5.

2 OBSERVATIONS

HD 171488 was observed, using the spectropolarimeter NARVAL at the Telescope Bernard Lyot, in 2007 from May 31 to June 13, and November 8 to 13 and in 2008 from May 26 to June 2. The observations cover the wavelength range from 370 to 1050 nm with a resolution of approximately 65 000. A total of 30, 14 and 16 circular polarization sequences were obtained, respectively, in 2007 May, 2007 November and 2008 May where each sequence comprises four individual sub-exposures takes in different polarimeter configurations. The journal of observations is shown in Table 1. In total, six nights were lost to poor weather conditions in 2008.

Table 1. Journal of observations for the data presented in this paper taken over three epochs: from 2007 May 21 to 26, 2007 November 8 to 13 and 2008 May 26 to 30. The rotational phases are computed using an ephemeris of 245 3526.5 (Jeffers & Donati 2008). Only the phase of the first sub-exposure is tabulated.

Date	JD 245 0000+	UT	Phase	Exposure time (s)	S/N
		2007 May			
2007 May 21	4242.48	23:18:01	0.460	4 × 600	279
2007 May 21	4242.51	24:01:52	0.482	4 × 600	278
2007 May 21	4242.54	0:45:17	0.505	4 × 600	268
2007 May 21	4242.62	2:46:41	0.568	4 × 600	324
2007 May 21	4242.65	3:30:06	0.591	4 × 600	336
2007 May 22	4243.48	23:26:15	1.212	4 × 600	178
2007 May 22	4243.51	24:09:40	1.234	4 × 600	207
2007 May 22	4243.54	0:53:06	1.257	4 × 600	173
2007 May 22	4243.57	1:36:53	1.280	4 × 600	110
2007 May 22	4243.60	2:20:18	1.302	4 × 600	165
2007 May 22	4243.63	3:03:43	1.325	4 × 600	197
2007 May 22	4243.66	3:37:32	1.346	4 × 300	170
2007 May 23	4244.48	23:23:10	1.958	4 × 600	254
2007 May 23	4244.51	24:06:35	1.981	4 × 600	315
2007 May 23	4244.54	0:50:01	2.003	4 × 600	338
2007 May 23	4244.56	1:23:52	2.025	4 × 300	240
2007 May 23	4244.58	1:47:17	2.037	4 × 300	252
2007 May 23	4244.60	2:10:41	2.049	4 × 300	248
2007 May 23	4244.61	2:34:06	2.061	4 × 300	204
2007 May 23	4244.63	2:57:31	2.073	4 × 300	224
2007 May 23	4244.64	3:20:56	2.086	4 × 300	239
2007 May 24	4245.50	0:10:32	2.731	2 × 600	96
2007 May 24	4245.56	1:37:22	2.776	2 × 600	104
2007 May 24	4245.59	2:11:14	2.799	4 × 600	226
2007 May 24	4245.62	2:54:40	2.822	4 × 600	314
2007 May 24	4245.65	3:38:04	2.844	3 × 600	206
2007 May 26	4247.55	1:08:16	4.257	4 × 600	317
2007 May 26	4247.58	1:51:41	4.279	4 × 600	351
2007 May 26	4247.61	2:35:06	4.302	2 × 600	347
		2007 November			
2007 November 8	4413.24	17:52:49	128.496	4 × 600	147
2007 November 8	4413.25	18:03:13	128.503	4 × 600	57
2007 November 8	4413.28	18:43:49	128.526	4 × 600	430
2007 November 8	4413.31	19:26:55	128.548	4 × 500	382
2007 November 9	4414.26	18:12:32	129.259	4 × 600	375
2007 November 9	4414.29	18:57:43	129.281	4 × 600	404
2007 November 10	4415.25	18:04:48	129.999	4 × 600	408
2007 November 10	4415.28	18:49:60	130.022	4 × 600	434
2007 November 11	4416.25	17:56:00	130.747	4 × 600	446
2007 November 11	4416.28	18:41:13	130.770	4 × 600	451
2007 November 12	4417.25	17:55:47	131.495	4 × 600	421
2007 November 12	4417.31	19:26:50	131.540	4 × 500	392
2007 November 13	4418.24	17:53:25	132.235	4 × 600	370
2007 November 13	4418.31	19:26:08	132.288	4 × 600	303
		2008 May			
2008 May 26	4613.46	22:57:40	0.919	4 × 300	85
2008 May 26	4613.48	23:28:46	0.934	4 × 450	33
2008 May 28	4615.56	1:16:14	2.487	4 × 300	324
2008 May 28	4615.57	1:40:30	2.500	4 × 300	290
2008 May 28	4615.59	2:04:12	2.512	4 × 300	314
2008 May 28	4615.61	2:27:53	2.524	4 × 300	322
2008 May 28	4615.62	2:51:33	2.537	4 × 300	320
2008 May 28	4615.64	3:15:15	2.549	4 × 300	319
2008 May 30	4617.48	23:30:23	3.928	4 × 300	290
2008 May 30	4617.5	23:53:49	3.924	4 × 300	279

Table 2. Summary of the fundamental parameters of HD 171488 used in this paper. The rotational period of Strassmeier et al. (2003) is used as it is derived from photometric data. The radius of Marsden et al. (2006) is used as it is derived from the absolute bolometric magnitude.

Parameter	Value	Source
Inclination	$60^\circ \pm 10^\circ$	This work
$v \sin i$	$37.5 \pm 0.5\,\mathrm{km\,s^{-1}}$	This work
Radial velocity	$-22.70 \pm 0.1\,\mathrm{km\,s^{-1}}$	This work – 2007 May
	$-22.60 \pm 0.1\,\mathrm{km\,s^{-1}}$	This work – 2007 November
Photospheric temperature	5808 K	Jeffers & Donati (2008)
Spot temperature	4200 K	Strassmeier et al. and Marsden et al.
Rotation period	1.3371 ± 0.0002 d	Strassmeier et al.
Radius	$1.15 \pm 0.08\,\mathrm{R}_\odot$	Marsden et al.

2.1 Data processing

The data were optimally extracted using the LIBRE ESPRIT package installed at the Telescope Bernard Lyot (TBL). This has been extensively used in the reduction of spectropolarimetric data. Further details can be found in Donati & Brown (1997). Telluric lines are also used to correct for any variations in the spectrograph as described by Jeffers et al. (2007).

The signal enhancement technique least-squares deconvolution (LSD) was applied to both Stokes *I* and *V* spectra. The list of spectral lines is obtained from the local thermodynamic equilibrium model atmospheres of Kurucz (1993) for $T_{\rm eff} = 5800$ K and $\log g = 4.5$. As shown by Jeffers et al. (2006), there is no significant difference between spherical (PHOENIX) and plane-parallel (ATLAS) atmospheres at the F9V/G0V spectral type. We used 4607 lines for 2007 May and 4663 for 2007 November and 2008 May. Spectral regions that contain lines not formed in the photosphere were also omitted. The velocity bin is 1.8 km s^{-1} per CCD pixel.

2.2 System parameters

The stellar parameters of HD 171488 were determined using the method of Jeffers & Donati (2008) and are summarized in Table 2. In comparison to the system parameters of Jeffers & Donati (2008), there is a slight variation, which we attribute to the improved instrumentation used in this analysis.

3 SURFACE IMAGES

The surface brightness images and magnetic field topology of HD 171488 were reconstructed using the maximum entropy code of Brown et al. (1991) and Donati & Brown (1997).

3.1 Surface brightness image

The two-component model of Collier Cameron (1992) is used to reconstruct the surface brightness images. In this model all spots have the same temperature, and contributions from the penumbrae are not included. A synthetic Gaussian line profile is used as the average intrinsic line profile. This template profile is scaled by 0.5 and 1.0 to represent the spotted and quiet photospheres, respectively.

The reconstructed images from the Stokes *I* data are shown in Fig. 1 for 2007 May, 2007 November and 2008 May, respectively. Given the short rotational phase covered by each observing run, we reconstruct the image for the complete data set. Each image is fitted to a χ^2 level of 0.15 for 2007 May and November and 0.3 for 2008 May, due to poorer data quality. The surface image

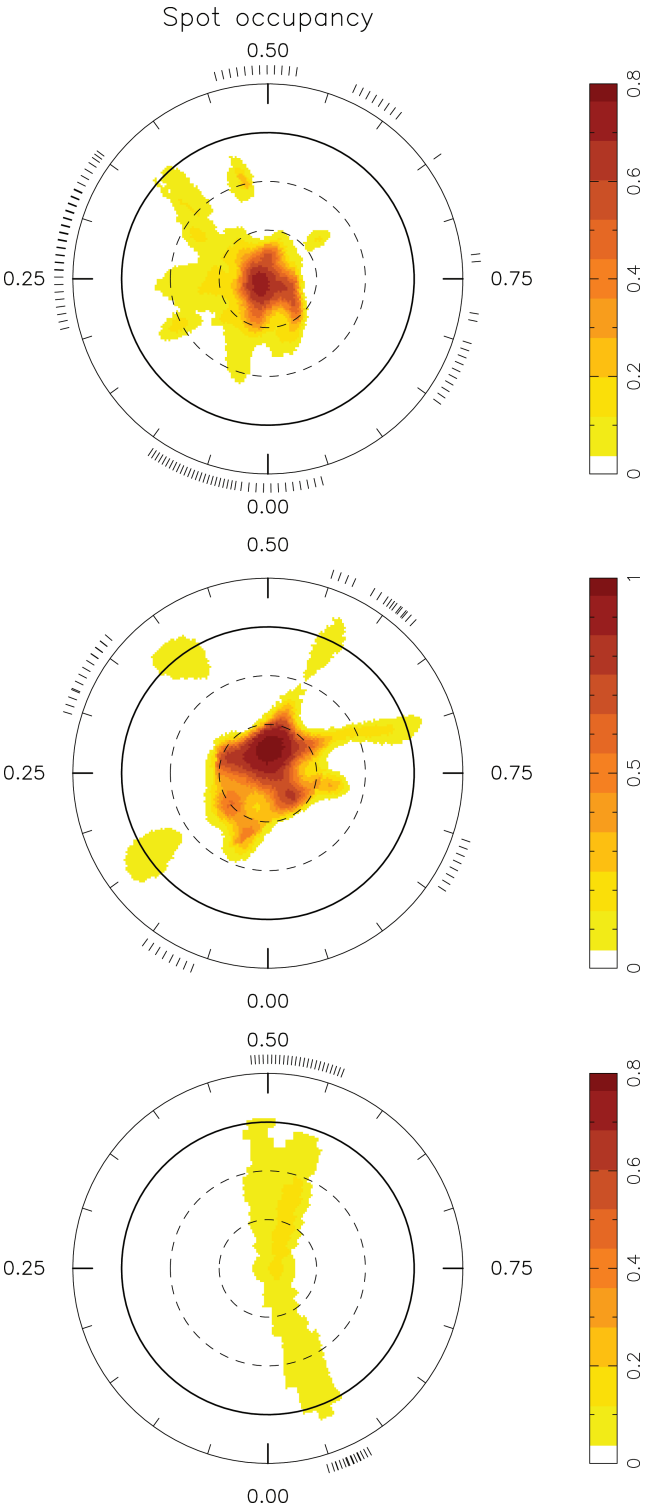

Figure 1. Maximum entropy brightness maps for HD 171488 in 2007 May (top), 2007 November (middle) and 2008 May (bottom). These images are flattened polar projections extending down to a latitude of -30°, where the bold line depicts the equator and the dashed lines are at 30° intervals. The radial ticks surrounding each image indicate the rotational phase of individual Stokes *I* observations. The images shown here include the values for differential rotation measured in Section 4 to avoid smearing of spots over the long phase coverage of our data sets.

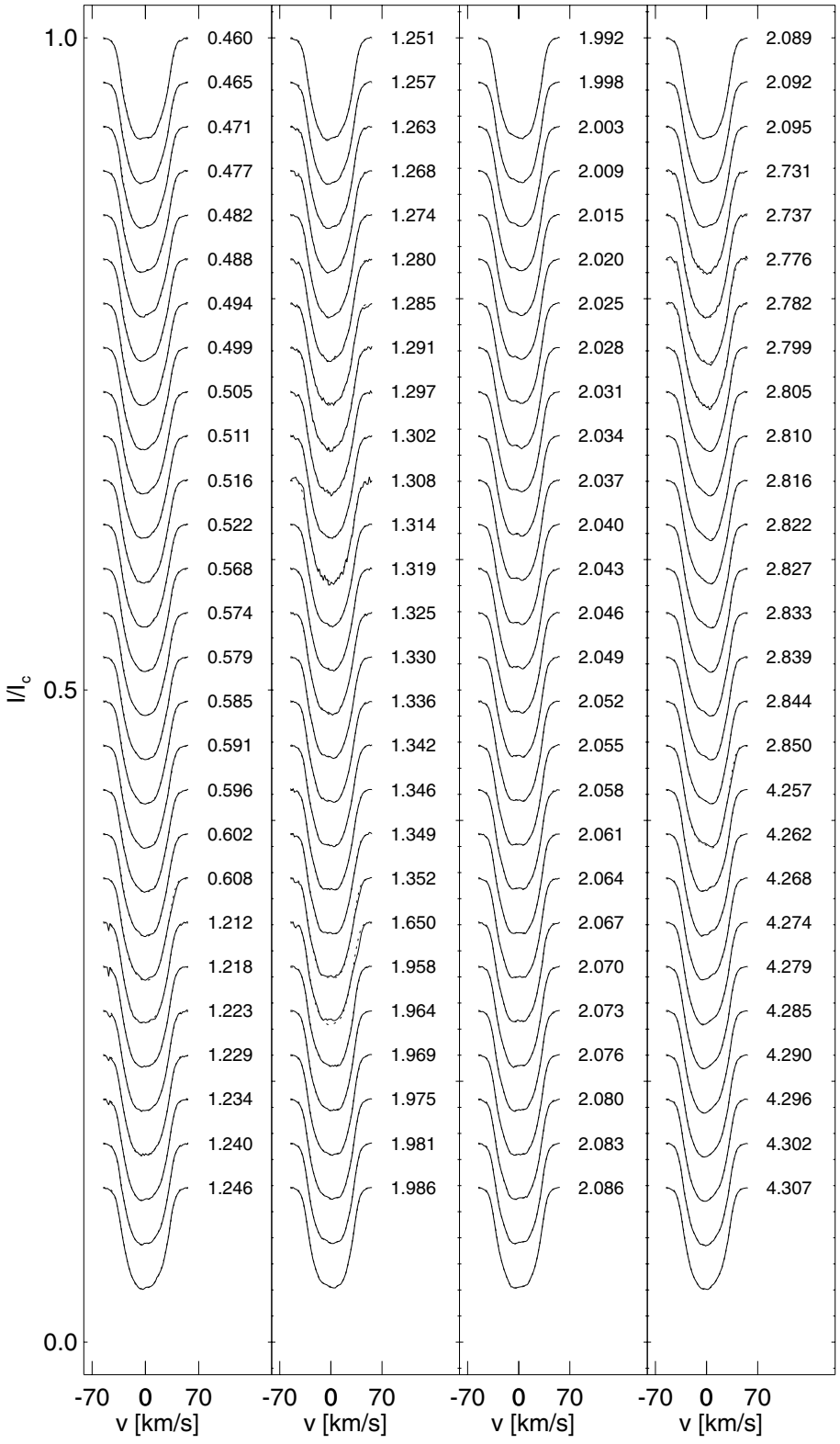

Figure 2. Maximum entropy fits (dashed line) to the Stokes *I* LSD profiles (solid line) for 2007 May. The rotational phase is shown to the right of each profile.

also incorporates the stellar differential rotation, as determined in Section 4 to account for the evolution of starspots over the time-span of the data set. The time series of profiles and corresponding maximum entropy-regulated fits to the data are shown in Figs 2 and 3, respectively.

The spot coverage is 8, 7 and 2 per cent for 2007 May, 2007 November and 2008 May, respectively. The surface brightness distributions of 2007 May and November are dominated by an extended polar cap and high-latitude spot coverage. The polar cap varies in strength and size between the two data sets, while also

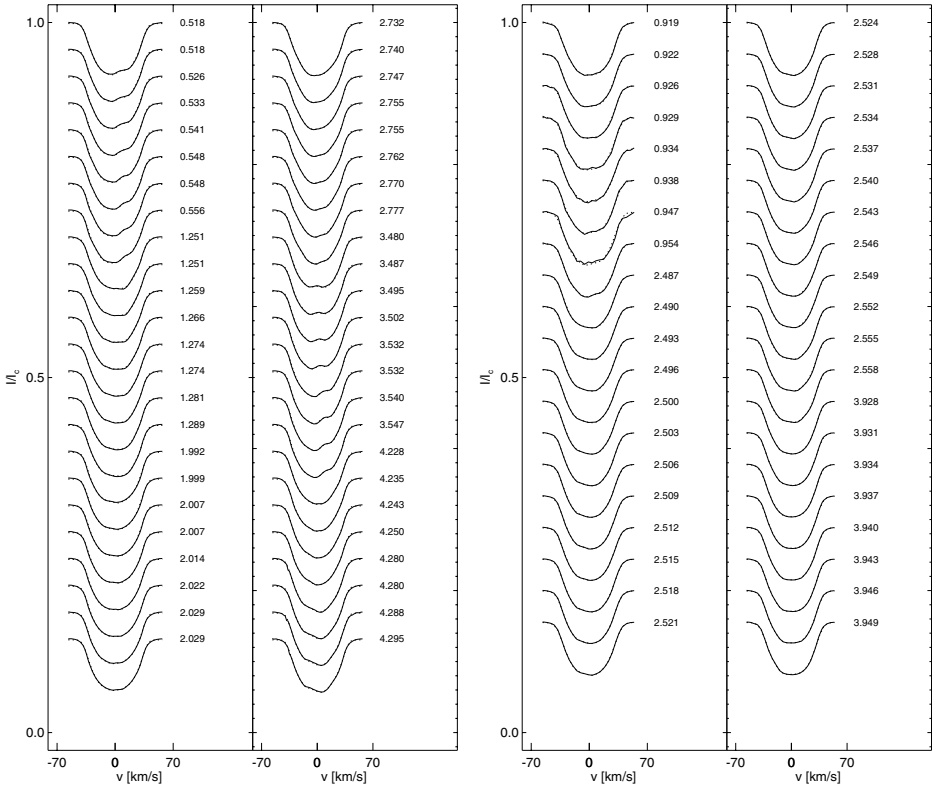

Figure 3. Maximum entropy fits (dashed line) to the Stokes *I* LSD profiles (solid line) for 2007 November (left) and 2008 May (right). The rotational phase is shown to the right of each profile.

drifting off-centre in 2007 November, to almost disappearing in 2008 May, though this probably results from the poor phase coverage of this epoch. The high-latitude spot features are more pronounced in 2007 November and 2008 May extending down to 45°, while high-latitude spots are weaker and less well defined in the 2007 May image. All maps show fragmented and weak low-latitude spot features with 2007 November showing a more concentrated spot feature at a phase of 0.5 and a latitude of 30°. The phase coverage is good for 2007 May and November but very poor for 2008 May, implying that for this epoch the constructed features are reliable only to a first approximation.

3.2 Latitudinal and longitudinal distribution of starspots

The fractional spot occupancy as a function of latitude is shown in Fig. 4 for 2007 May and November and is calculated using the equation

$$F(l) = \frac{S(l)\cos(l)\,\mathrm{d}l}{2}, \tag{1}$$

where $F(l)$ is the fractional spottedness at latitude l and $S(l)$ is the average spot occupancy at latitude l. The cos (l) is included to account for fewer pixels at the poles in the ZDI code. The resulting plots (Fig. 4) show that the starspot coverage is predominantly at polar and high latitudes for both epochs. The fractional spot coverage is also determined as a function of longitude integrated over latitude from 0° to 90° and 0° to 60°, and shown in Fig. 5, to enable the comparison of the surface brightness images of this analysis with published photometric light curves.

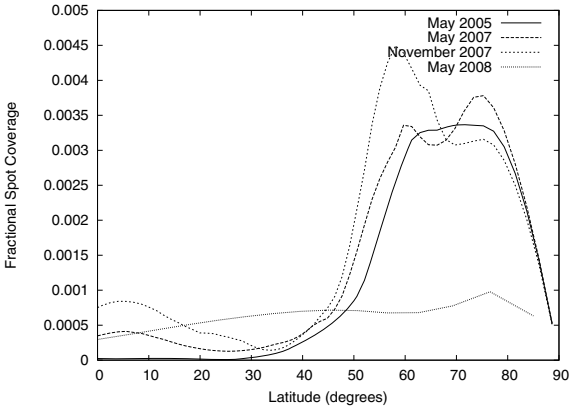

Figure 4. Fractional spot coverage per latitude bin integrated over longitude for all epochs of this analysis. For comparison, the fractional spottedness is also shown for 2005 May.

3.3 Surface magnetic field topology

The reconstruction of the magnetic field topology assumes the weak magnetic field approximation and that the local flux profile remains constant over the stellar disc. Gaussians are used to model the local line profile. To determine the spatial distributions of radial, meridional and azimuthal magnetic field components, they are weighted by potential surface inhomogeneities in local magnetic field occupancy and the central depth of the intrinsic profile.

The reconstructed large-scale magnetic field topology for HD 171488 is shown in Fig. 6 for the three epochs of this analysis. The maximum entropy fits to the profiles, which were fitted to the noise levels (i.e. $\chi^2 = 0.9$–1.0), are shown in Figs 7 and 8.

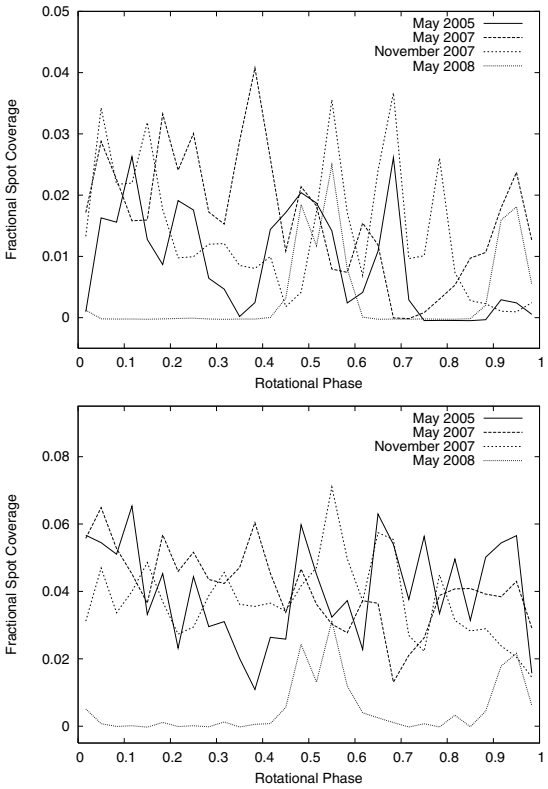

Figure 5. Fractional spot coverage per longitude bin integrated over latitude from 0° to 60° (top plot) and 0° to 90° (bottom plot) for 2004 September, 2005 May, 2007 May, 2007 November and 2008 May. These plots show that there is no evidence for active longitudes on HD 171488.

The quadratic magnetic flux, i.e. the local field modulus times the local relative surface area, for each of the epochs is 70, 75 and 43 G, respectively, for 2007 May, 2007 November and 2008 May.

At all epochs, the overall polarities of the radial and azimuthal field distributions remained constant showing no evidence for the magnetic field reversal observed in τ Boo. There is insufficient phase coverage in 2008 May to reliably conclude that there is no positive radial field present. The majority of the magnetic flux is stored in the form of an azimuthal component for 2007 May, 56 per cent, and 2007 November, 70 per cent, and in the radial component for 2008 May, 54 per cent. The predominating feature of the azimuthal magnetic flux distribution is the permanent ring of the anticlockwise field surrounding the rotational pole. However, the location and shape of the ring can be seen to evolve over the time-span of our data sets. In 2007 May, the ring is exactly centred around the pole, extending down to 60°, with a closed ring of flux, while in November the ring is slightly off-centred, open and extends down to 45°. In 2008 May, the poor phase coverage can only give a slight indication that the anticlockwise field dominates around the rotational pole. At lower latitudes, a positive magnetic field dominates in 2007 May while a negative field dominates in 2007 November.

The radial magnetic field comprises 40 per cent (2007 May) and 21 per cent (2007 November) of the magnetic energy (e.g. $\frac{B_r^2}{B_{\rm tot}^2}$). At all epochs, it is dominated by large regions of negative magnetic field features, with small isolated regions of the positive field at all latitudes. The magnetic field topology for 2007 November shows an extended positive feature of the positive field though since it is at a region without phase coverage, its reliability is not certain. The meridional component shows only weak mixed polarity magnetic field structures at the rotational pole at all epochs. The field orientation remains constant and results from the high-latitude toroidal field ring. However, it should be noted that ZDI is not sensitive to reconstructing a meridional field at low latitudes.

4 DIFFERENTIAL ROTATION

To determine the temporal evolution of differential rotation over the epochs of this analysis, we use the sheared image method of Petit, Donati & Collier Cameron (2002). The basic concept of the method is that the stellar differential rotation is incorporated into the image reconstruction process. The rotation rate Ω depends on latitude according to the simplified solar-like differential rotation law:

$$\Omega(\theta) = \Omega_{\rm eq} - \delta\Omega \sin^2\theta, \tag{2}$$

where $\Omega(\theta)$ is the rotation rate at colatitude θ, $\Omega_{\rm eq}$ is the equatorial rotation rate and $\delta\Omega$ is the difference between polar and equatorial rotation rates. A grid of values for $\Omega_{\rm eq}$, $\delta\Omega$ is then computed, where for each permutation of $\Omega_{\rm eq}$, $\delta\Omega$ the image reconstruction code is converged to a fixed value of the spot filling factor for Stokes *I* data and the quadratic magnetic flux for Stokes *V* data. The goodness of fit measured by χ^2 for each model is then plotted as a χ^2 landscape plot. Given the phase coverage of the data sets, it was only possible to measure the differential rotation for HD 171488 in 2007 May and November.

4.1 Stokes *I* data

For the Stokes *I* data, the imaging code was converged to spot coverage values of 8 per cent in 2007 May and 7 per cent in 2007 November. This value was obtained from a reconstruction of the surface brightness image. As we require only the total spot coverage, it is not necessary to include an accurate value of the differential rotation. The resulting χ^2 landscape for 2007 May is shown in Fig. 9. The parameters that best fit the paraboloid are summarized in Table 3.

4.2 Stokes *V* data

Likewise, we determine the differential rotation for Stokes *V* data by converging each value on the $\Omega_{\rm eq}$–dΩ plane to a fixed value of 70 and 75 G, respectively, for 2007 May and November. The parameters that best fit the paraboloid shown in Fig. 10 are also summarized in Table 3.

5 DISCUSSION

5.1 Surface brightness distributions

The surface features reconstructed with this data set are of much higher resolution than those of our previous results of HD 171488 (Jeffers & Donati 2008) observed in 2005 May using the Musicos spectropolarimeter. The surface brightness distributions are dominated by a long-lived polar cap and short-lived low- to high-latitude features. Between the first two epochs of this analysis (i.e. over 138 d), there is no similarity of the starspots suggesting that it is incorrect to use data sets that span more than the lifetime of the starspots, for example, as was shown by Savanov & Strassmeier (2008) for the K0 dwarf star HD 291095.

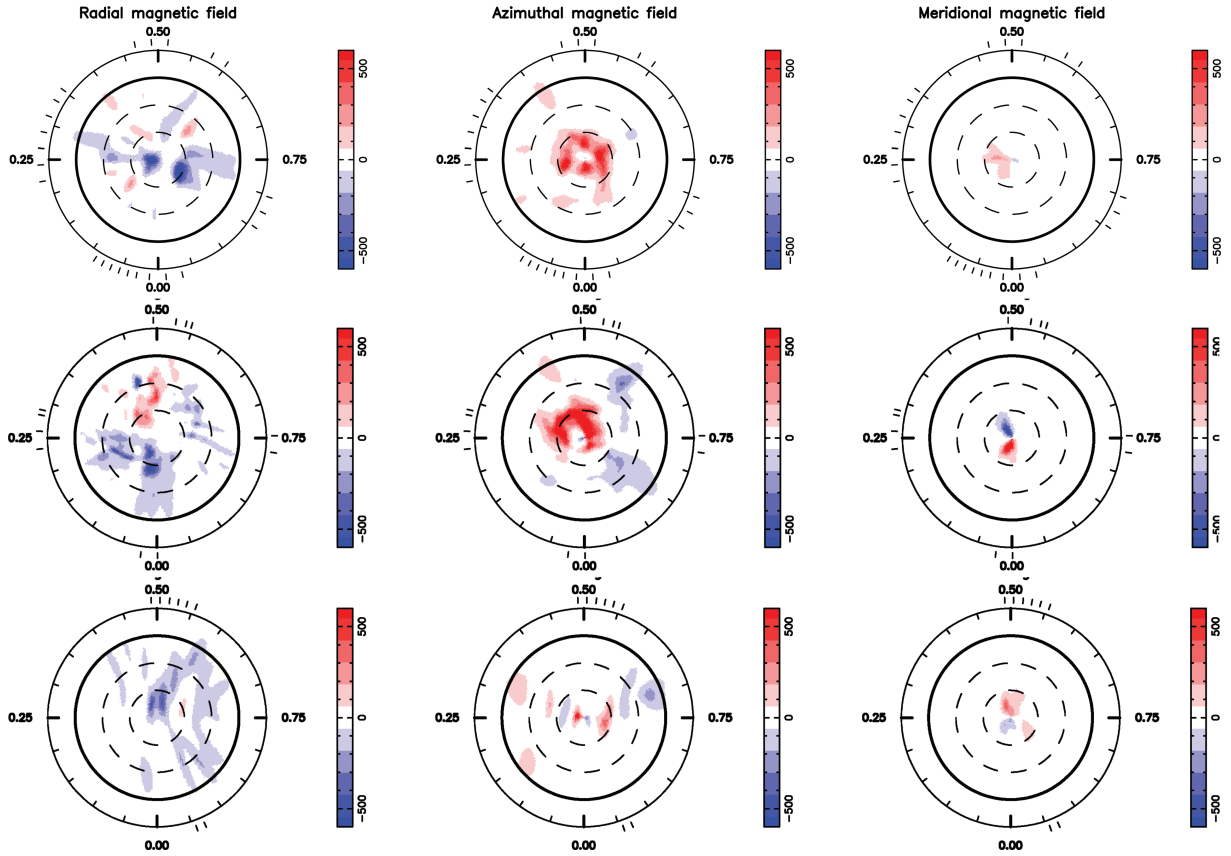

Figure 6. Maximum entropy magnetic maps for HD 171488 in 2007 May (top), 2007 November (middle) and 2008 (bottom) in the same format as the brightness maps. The scale of the magnetic field strengths are in Gauss, where positive field values correspond to magnetic vectors directed outwards, anticlockwise and polewards, respectively, for radial, azimuthal and meridional field components. The images shown here include the values for differential rotation measured in Section 4 to avoid smearing of magnetic features over the long phase coverage of our data set.

5.1.1 Active longitudes

The fractional spot occupancy as a function of longitude is shown in Fig. 5 which clearly shows that there are no active longitudes on HD 171488. In Fig. 5, we have also included the data from 2004 September (Marsden et al. 2006) and 2005 May (Jeffers & Donati 2008). This is in direct contrast to the results of Järvinen et al. (2008), where they show that for 2007.39 (i.e. 2007 May) HD 171488 should have a primary spot at a phase of −0.014 and a secondary spot at a phase of 0.681. The corresponding epoch of our analysis, i.e. 2007 May, shows no indication of large spot concentrations at these phases.

The observations of Järvinen et al. (2008) for epoch 2007.39 also span a time period of 66 d from JD 2454207 to 245483. As discussed by Barnes et al. (2001), the long-term stability of high, mid and low latitudes for the G2V star He699 has been shown to vary on a time-scale that is shorter than the temporal spacing of their observations. This could imply that their observations do not accurately reconstruct the spot distribution, particularly because of the high differential rotation of HD 171488 that we have measured in this work and in Jeffers & Donati (2008).

The reliability of reconstructed 'active longitudes' has been investigated recently by Jeffers & Keller (2009) for the case of single stars. In this paper, a simple analytical model is used to calculate the light curve of a star with an arbitrary spot pattern to show that active longitudes are a likely consequence of the limited information content of a light curve. Indeed, our reconstructed surface brightness images show no resemblance to those of Järvinen et al. (2008) for the same epoch.

To attempt to explain the discrepancy between the two results, we have constructed some simple models. Using the light-curve inversion code DOTS (Collier Cameron 1997), the surface brightness distribution of 2007 November was used to generate a synthetic light curve, comprising 500 points with uniform sampling and with random Gaussian noise (0.004) being added to match the standard photometric precision of ground-based telescopes (Fig. 11: middle panel). The resulting light curve, from the modelled distribution of spots, was used as input to DOTS to reconstruct the surface brightness distribution using the maximum entropy χ^2 minimization method (Collier Cameron 1997). The resulting surface brightness distribution is shown in Fig. 11 (top-right panel). The presence of one large spot and a smaller spot approximately 180° apart, and joined by weaker spot coverage, is because the inversion of a star's light curve is an ill-posed problem with an infinite number of solutions that can be found to fit the data. The modelled light curve is then inverted to give a surface brightness distribution with clear spot groupings that directly correspond to the number of minima in the photometric light curve.

5.1.2 Latitudinal distribution

The distribution of starspots as a function of latitude is shown in Fig. 4 for all epochs of this analysis. For comparison, the plot also includes epochs of 2004 September and 2005 June. The latitudinal

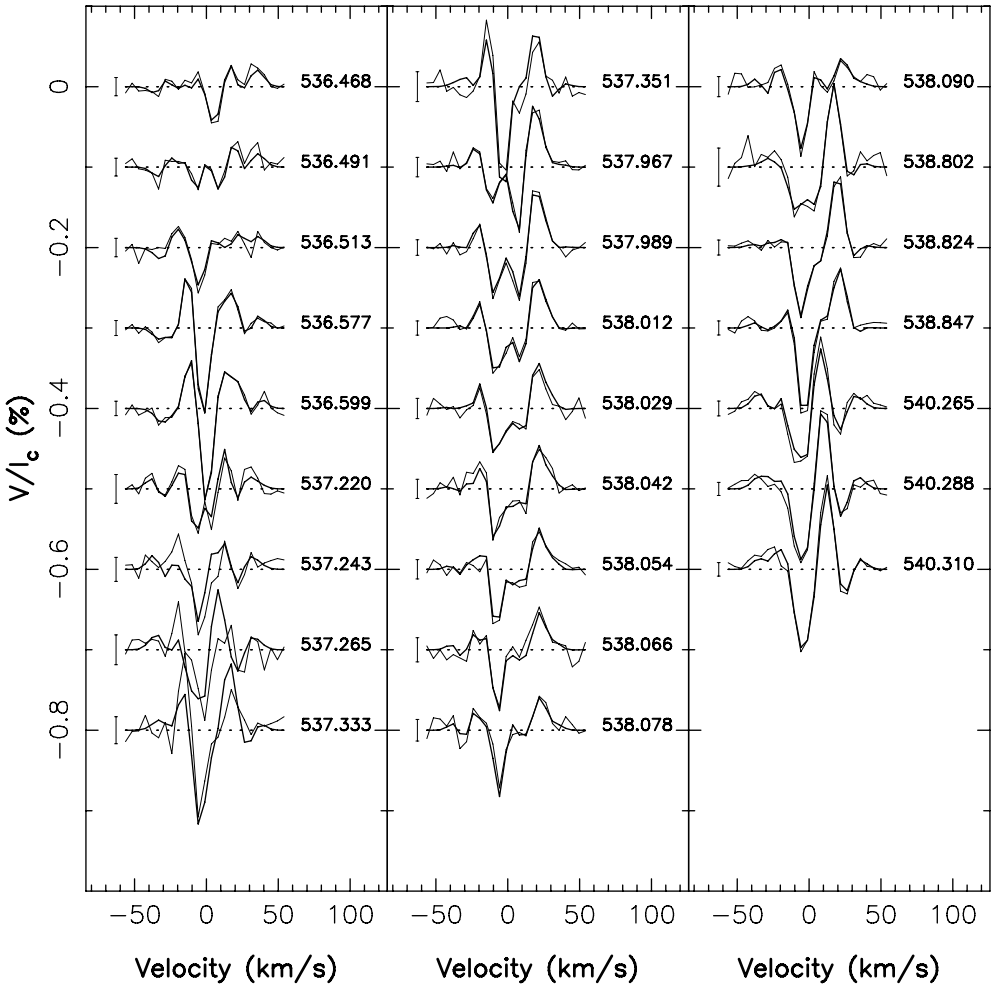

Figure 7. Maximum entropy fits (bold line) to the Stokes *V* LSD profiles (solid line) for 2007 May. The rotational phase is shown to the right of each profile. The length of the vertical bar on the left-hand side of the profile is the size of the error bar.

distribution clearly shows predominantly polar and high-latitude spots at all epochs with little low-latitude spot coverage reconstructed even at epochs with good phase coverage. This is in good agreement with the surface maps of HD 171488 reconstructed by Strassmeier et al. (2003), Huber et al. (2009) and Marsden et al. (2006), even though only Marsden et al. (2006) used LSD. We find that there is no apparent temporal evolution of the latitude distribution of spots.

Theoretical efforts to understand the formation of polar caps have resulted in several recent theoretical models where the accumulation of magnetic flux at high latitudes can result from the poleward deflection of emerging flux tubes by the Coriolis force (e.g. Schüssler & Solanki 1992; Schüssler et al. 1996; Granzer et al. 2000), or using meridional flows to sweep magnetic flux from decaying active regions up towards the poles (Schrijver & Title 2001). Polar caps have also been directly detected by Jeffers et al. (2005) for the primary star of the eclipsing binary SV Cam.

5.2 How does a shallow convection zone affect magnetic field topology?

The large-scale magnetic field topology comprising radial, azimuthal and meridional components has been reconstructed for three epochs. The majority of the magnetic energy is in the form of an azimuthal (toroidal) field for 2007 May and November with 56 and 70 per cent, respectively, and in the form of a radial field for 2008 May with 54 per cent.

As with previous magnetic maps, the dominating feature is the strong ring of the positive magnetic field, which is located around the rotational axis in 2007 May and slightly off-centred in 2007 November. The ring of the azimuthal field is commonly observed in the magnetic field distributions of late-type stars such as AB Dor (Donati et al. 2003a), where it has been consistently reconstructed over a 10-yr period, HR 1099, where a double-ring structure has been observed and the planet-hosting star τ Boo where a polarity switch has been observed over a 1-yr interval (Catala et al. 2007; Donati et al. 2008; Fares et al. 2009). These large-scale azimuthal rings have not been observed on the fully convective stars AD Leo, EV Lac, YZ Cmi and EQ Peg A (Morin et al. 2008). Positive azimuthal magnetic field features dominate at all latitudes in 2007 May, while the negative field dominates at low latitudes in 2007 November. The existence of the large-scale azimuthal magnetic field is considered to be evidence of a non-solar-type dynamo operating in these stars, which is supported by theoretical models of dynamo action in rapidly rotating solar-type stars (Brown et al. 2007). These models show that for rapidly rotating solar-type stars, with a rotation rate three times greater than solar, the global scale toroidal and poloidal magnetic fields can be generated and maintained in the

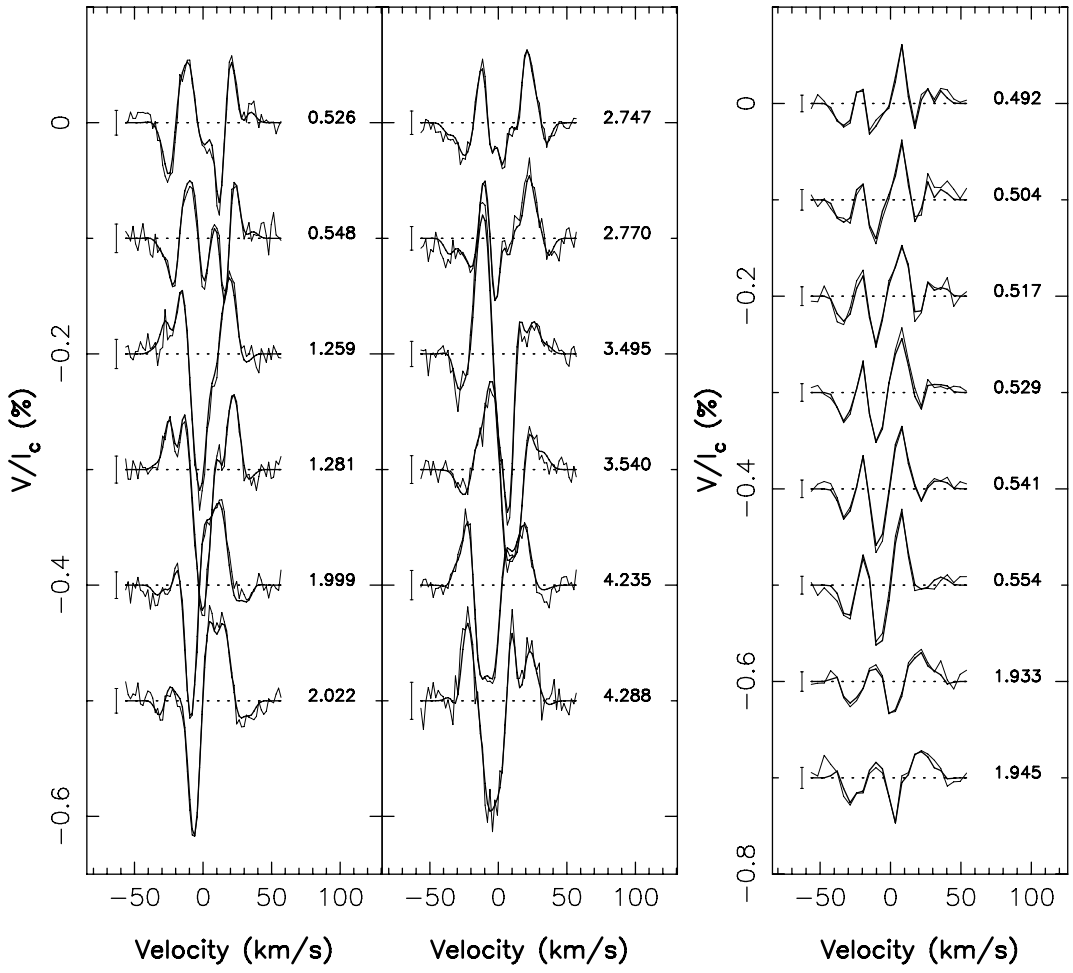

Figure 8. Maximum entropy fits (bold line) to the Stokes *V* LSD profiles (solid line) for 2007 November (right-hand plot) and 2008 May (left-hand plot). The rotational phase is shown to the right of each profile. The length of the vertical bar on the left-hand side of the profile is the size of the error bar.

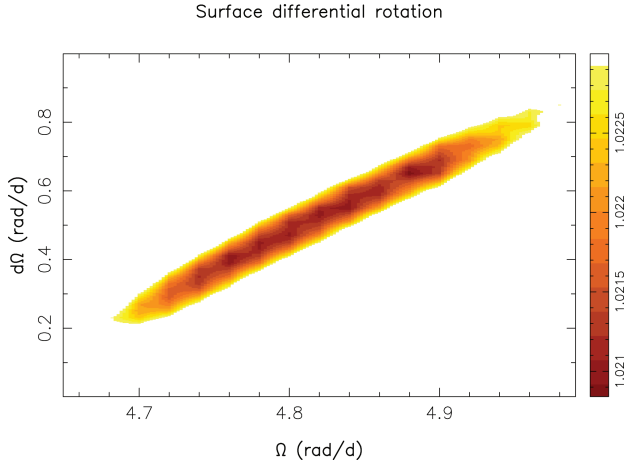

Figure 9. Differential rotation landscape plot for HD 171488 in 2007 May, where each permutation in the Ω_{eq}–dΩ space was converged to a spot coverage of 8 per cent. The outer ellipse corresponds to the 1.5σ confidence interval.

Table 3. Differential rotation results for 2007 May and November. For comparison, the results obtained by Jeffers & Donati (2008) in 2005 June and by Marsden et al. (2006) in 2004 September are also shown.

Epoch	Ω_{eq} (rad d^{-1})	dΩ (rad d^{-1})	No of data points	Reference
		Stokes *I* data		
2004.65	4.786 ± 0.013	0.402 ± 0.044		M(2006)
2005.42	4.93 ± 0.05	0.52 ± 0.04	4200	J & D (2008)
2007.39	4.79 ± 0.09	0.4 ± 0.15	6867	This work
2007.77	4.86 ± 0.03	0.41 ± 0.02	3072	This work
		Stokes *V* data		
2005.42	4.85 ± 0.05	0.47 ± 0.04	1125	J & D (2008)
2007.39	4.78 ± 0.027	0.45 ± 0.053	625	This work
2007.77	4.79 ± 0.08	0.415 ± 0.016	768	This work

convection zone without requiring a tachocline of shear to build up the strong large-scale toroidal fields. For the case of the Sun, large-scale toroidal fields have only emerged in simulations where a tachocline has been included (Browning et al. 2006) to store the large-scale magnetic fields. However, the models of Brown et al. (2007) would confirm that a non-solar-type dynamo is operating in these stars. The field distribution and orientation also serve as an important diagnostic to study and explain spot lifetimes based on numerical studies (Işik, Schüssler & Solanki 2007).

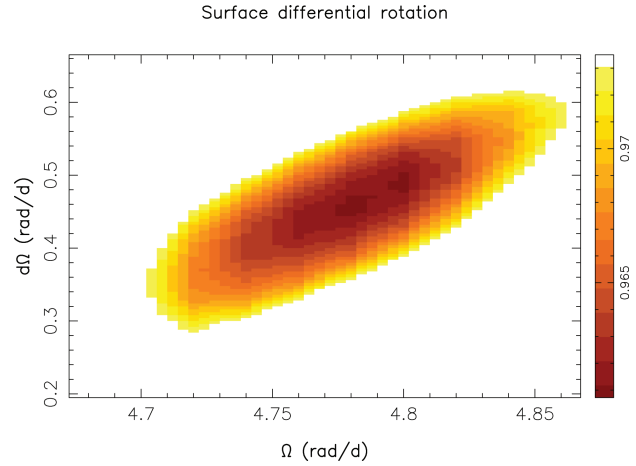

Figure 10. Differential rotation landscape plot for HD 171488, where each permutation in the Ω_{eq}–dΩ space was converged to 70 G for 2007 May.

The radial magnetic field is primarily in the form of large negative field concentrations, which extend to equatorial latitudes, with small amounts of positive field distributed at all latitudes. This is consistent with the results reconstructed for HD 171488 in 2005 May (Jeffers & Donati 2008) and in 2004 September (Marsden et al. 2006). The presence of both negative and positive fields at high latitudes has also been observed on other late-type stars such as AB Dor and LQ Hya (Donati et al. 2003a), but is inconsistent with models of the emergence of magnetic flux on the Sun and how it is transported polewards. Magnetic flux transport simulations have been modelled by Mackay et al. (2004) to determine how these mixed polarity patterns can arise on rapidly rotating stars. To produce the observed polarity patterns, they show that it is necessary to have a flux emergence rate 30 times greater than solar, a flux emergence between 50° and 70° and a meridional flow of 100 m s^{-1}. The observed radial field distribution on HD 171488 is further evidence for non-solar flux generation emergence and transport on young rapidly rotating stars.

5.3 How does a shallow convection zone affect differential rotation?

The differential rotation measurements of this analysis confirm the results of Jeffers & Donati (2008), where HD 171488 was found to have the highest differential rotation measured using Zeeman–Doppler imaging techniques. As discussed by Jeffers & Donati (2008), this result does not fit the predicted differential rotation derived for spectral type G0V from Doppler imaging (Barnes et al. 2005), chromospheric monitoring (Donahue, Saar & Baliunas 1996) and broad-band photometry (Henry et al. 1995). With a value of differential rotation that is nine and 10 times greater than solar, it is almost twice as large as the differential rotation measured for the other early G dwarfs LQ Lup (Donati et al. 2000) and R58 (Marsden et al. 2005) using similar measurement techniques. The results measured for differential rotation are in agreement with those measured for the F7V planet-hosting star τ Boo. This high value of differential rotation is in contrast to the result of Huber et al. (2009) where they conclude that HD 171488 has rigid rotation. However, their results are based on very noisy line profiles, and that the minima of the photometric light curves did not evolve with time. However as shown by Jeffers & Keller (2009), light-curve evolution does not depend on the star's differential rotation rate.

Another significant result is that the differential rotation measurement using Stokes *I* and *V* data is consistently the same over three epochs. Other long-term measurements of differential rotation using Stokes *I* and *V* data have been made for the K0 dwarf AB Dor (Donati et al. 2003b), where there is a large variation between differential rotation measured using Stokes *I* and *V* data. Donati et al. (2003b) interpret this as evidence of a non-solar-type dynamo where the magnetic regions are not anchored at the same depth in the convective zone and therefore do not experience the same shear. Given that HD 171488 has a very shallow convective zone, our result that Stokes *I* and *V* differential rotation measurements are the same can be further evidence for a non-solar-type dynamo operating in young active solar-type stars.

Including the results of Marsden et al. (2006) and Jeffers & Donati (2008), it is clear that there is no evidence for the temporal evolution of differential rotation in either the Stokes *I* or Stokes *V* data sets from 2004 September to 2007 November. This result is in contrast to the long-term analysis of AB Dor, where Jeffers et al. (2007) and Donati et al. (2003b) found that differential rotation measurements, using Stokes *I* and *V* data, show variations on a time-scale of at least 1 yr.

5.4 How do shallow convective zones impact dynamo processes?

The observation of the signatures of dynamo processes in late-type stars allows a more in-depth understanding of the fundamental dynamo processes that are well established in the case of the Sun. These observations are important to understand how solar dynamo theories depend on basic stellar parameters such as the star's convective zone depth and (differential) rotation rate. In particular, the observation of stars with shallow convective zone depths, considered in this work to be stars with spectral types earlier than solar, allows an understanding of the importance of the tachocline in dynamo processes.

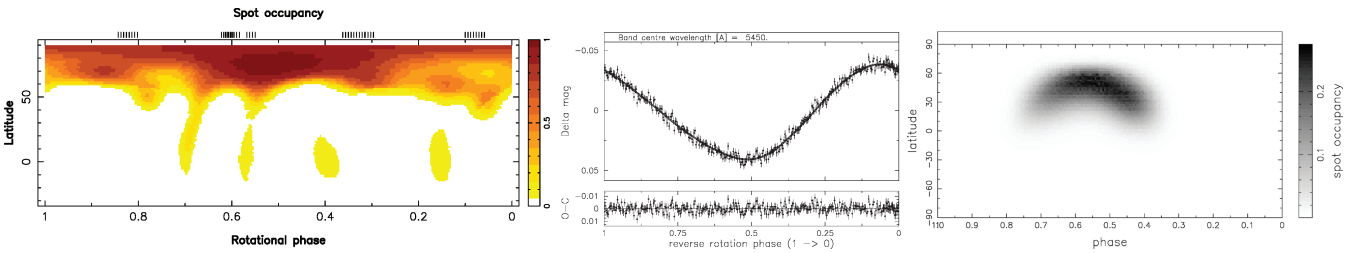

Figure 11. The original spot distribution (left) of HD 171488 reconstructed using Doppler imaging for 2007 November (Fig 1:middle panel). This was used as input to the light-curve modelling program DOTS, from which the light curve shown in the middle panel was computed. This light curve was then used as the only input to the light-curve inversion code. The reconstructed surface brightness image from the light curve is shown to the right.

Table 4. Comparison of fundamental stellar parameters of HD 171488 and τ Boo as determined from the stellar evolution models of Siess et al. (2000). The input parameters (temperature, radius and mass) for τ Boo are taken from Fuhrmann et al. (1998).

Star	Age (Myr)	Temp (K)	Period (d)	Radius ($R_\odot$)	Mass ($M_\odot$)	Con zone depth $R_\odot$ (R_*)	Con zone mass $M_\odot$ (M_*)	Con turnover (yr)	Rossby no
HD 171488	30	5808	1.31	1.13	1.2	0.233 (0.206)	7.06×10^{-3} (5.88×10^{-3})	0.0308	0.116
τ Boo	1120	6360	3/4	1.48	1.42	0.164 (0.108)	2.61×10^{-4} (1.86×10^{-4})	7.63×10^{-3}	1.07

The shrinking of the star's convection zone will effect both thin shell dynamos and distributed dynamos in different ways. For both the traditional solar 'thin shell' dynamos and distributed dynamos, the properties of the base of the convection zone and the role of the tachocline play an essential role due to the subadiabatic stratification in the overshoot region and the strong radial shear of the tachocline. Thin shell dynamo models depend strongly on the properties of this region, as this is where they generate magnetic fields, while distributed dynamos are less effected (e.g. Guerrero & de Gouveia Dal Pino 2007).

Other dynamo models include that of Brown et al. (2007), where the global poloidal and toroidal magnetic fields can be generated and maintained in the convection zone, and the dynamo model of Spruit (2002), which only requires a sufficiently powerful differential rotation, which is measured for HD 171488 and τ Boo, and an internal instability in the toroidal magnetic field to provide new poloidal components. This results in a small-scale magnetic field which is produced in the radiative core with differential rotation as the dynamo's energy source and results in a predominantly azimuthal field.

As shown by Goudard & Dormy (2008), the depth and geometry of the convective zone can strongly impact the nature of the dynamo waves that are produced. This work shows that varying the aspect ratio (ratio of the radius of the inner bounding sphere to the radius of the outer bounding sphere) of the active dynamo region can make a sharp transition from dipole-dominated large-scale fields, like the geodynamo and which has been observed by Donati et al. (2008) in the fully convective star V374 Peg, to a cyclic dynamo with a weaker dipole/complex magnetic field, as has been observed in stars with shallow convective zones such as HD 171488 and τ Boo. Indeed, Donati & Landstreet (2009) conclude that for very active stars with a Rossby number of <1, stars with a mass of >0.5 $M_\odot$ show a strong to dominating azimuthal field mostly with a non-axisymmetric poloidal component.

One of the strongest signatures of the dynamo regeneration process is the reversal of the magnetic field. This has only been observed on the Sun and the F9V star τ Boo with a period of 2 yr (Catala et al. 2007; Donati et al. 2008). In contrast, since 2004 September, the azimuthal field ring of HD 171488 has not changed polarity implying that it has a cycle of at least 8 yr. Given its shorter rotation period (1.31 d), HD 171488 is much more active than τ Boo ($p = 3/4$ d), but despite this both stars have similarly high levels of differential rotation that does not show any temporal evolution. However, differences between the two stars can be seen in terms of the convective turnover time (Hurley, Tout & Pols 2002) and age. As is shown in Table 4, HD 171488 is slightly cooler and has a thicker convective zone. The convective turnover time, and consequently the efficiency of magnetic field generation or Rossby number, varies very quickly (by a factor of 10) with mass going from F7 to G0 spectral type. The smaller Rossby number for HD 171488 indicates that Coriolis forces are strong enough to influence convection. Both stars are main-sequence stars, though HD 171488 (30-Myr old; Siess, Dufour & Forestini 2000) is going through the last stage of contraction before arriving on the zero-age main sequence (refer to table 4). In contrast, τ Boo is 1.12-Gyr old (Fuhrmann, Pfeiffer & Bernkopf 1998; Siess et al. 2000) and is a middle-aged main-sequence star.

The cyclic period of the magnetic cycles on τ Boo is consistent with the Mount Wilson observations of chromospheric activity (Baliunas et al. 1995) where 40 per cent of their sample of approximately 100 K to F stars were observed to show cyclic behaviour with periods between 2.5 and 40 yr. The chromospheric activity shows a consistent relation with the inverse of the star's rotation rate, but breaks down for very active stars, with Rossby number $=$ 0.3 (e.g. for HD 171488 which has a Rossby number $= 0.1$).

Further observations of stars of similar and earlier spectral types to HD 171488 and τ Boo will increase our understanding of how dynamo processes change when the convective zone becomes very shallow and if there is a sudden change in the dynamo cycle period with decreasing convective zone depth.

ACKNOWLEDGMENTS

The authors would like to thank the TBL telescope operations team. SVJ currently acknowledges support from De Nederlandse Organisatie voor Wetenschappelijk Onderzoek (NWO).

REFERENCES

Baliunas S. et al., 1995, ApJ, 438, 269
Barnes J. R., Collier Cameron A., James D. J., Steeghs D., 2001, MNRAS, 326, 1057
Barnes J. R., Cameron A. C., Donati J.-F., James D. J., Marsden S. C., Petit P., 2005, MNRAS, 357, L1
Brown S. F., Donati J.-F., Rees D. E., Semel M., 1991, A&A, 250, 463
Brown B. P., Browning M. K., Brun A. S., Miesch M. S., Nelson N. J., Toomre J., 2007, in Stancliffe R. J., Dewi J., Houdek G., Martin R., Tout Christopher A., eds, AIP Conf. Ser. Vol. 948, Unsolved Problems in Stellar Physics: A Conference in Honor of Douglas Gough, Strong Dynamo Action in Rapidly Rotating Suns. Am. Inst. Phys., New York, p. 271
Browning M. K., Miesch M. S., Brun A. S., Toomre J., 2006, ApJ, 648, L157
Catala C., Donati J.-F., Shkolnik E., Bohlender D., Alecian E., 2007, MNRAS, 374, L42
Collier Cameron A., 1992, in Byrne P. B., Mullan D. J., eds, Surface Inhomogeneities on Late-type Stars (Invited Review), Modelling Stellar Photospheric Spots Using Spectroscopy. Springer-Verlag, Berlin, p. 33
Collier Cameron A., 1997, MNRAS, 287, 556
Donahue R. A., Saar S. H., Baliunas S. L., 1996, ApJ, 466, 384
Donati J.-F., Brown S. F., 1997, A&A, 326, 1135
Donati J., Landstreet J. D., 2009, ARA&A, 47, 333
Donati J.-F., Mengel M., Carter B., Marsden S., Collier Cameron A., Wichmann R., 2000, MNRAS, 316, 699
Donati J.-F. et al., 2003a, MNRAS, 345, 1145
Donati J.-F., Collier Cameron A., Petit P., 2003b, MNRAS, 345, 1187
Donati J. et al., 2008, MNRAS, 390, 545
Donati J.-F. et al., 2008, MNRAS, 385, 1179

Fares R. et al., 2009, MNRAS, 398, 1383
Fuhrmann K., Pfeiffer M. J., Bernkopf J., 1998, A&A, 336, 942
Goudard L., Dormy E., 2008, Europhys. Lett., 83, 59001
Granzer T., Schüssler M., Caligari P., Strassmeier K. G., 2000, A&A, 355, 1087
Guerrero G., de Gouveia Dal Pino E. M., 2007, A&A, 464, 341
Henry G. W., Eaton J. A., Hamer J., Hall D. S., 1995, ApJS, 97, 513
Huber K. F., Wolter U., Czesla S., Schmitt J. H. M. M., Esposito M., Ilyin I., González-Pérez J. N., 2009, A&A, 501, 715
Hurley J. R., Tout C. A., Pols O. R., 2002, MNRAS, 329, 897
Işik E., Schüssler M., Solanki S. K., 2007, A&A, 464, 1049
Järvinen S. P., Korhonen H., Berdyugina S. V., Ilyin I., Strassmeier K. G., Weber M., Savanov I., Tuominen I., 2008, A&A, 488, 1047
Jeffers S. V., Donati J.-F., 2008, MNRAS, 390, 635
Jeffers S. V., Keller C. U., 2009, in Stempels E., ed., AIP Conf. Ser. Vol. 1094, An Analytical Model to Demonstrate the Reliability of Reconstructed 'Active Longitudes'. Am. Inst. Phys., New York, p. 664
Jeffers S. V., Cameron A. C., Barnes J. R., Aufdenberg J. P., Hussain G. A. J., 2005, ApJ, 621, 425
Jeffers S. V., Aufdenberg J. P., Hussain G. A. J., Cameron A. C., Holzwarth V. R., 2006, MNRAS, 367, 1308
Jeffers S. V., Donati J.-F., Collier Cameron A., 2007, MNRAS, 375, 567
Kurucz R. L., 1993, CDROM 13 (ATLAS9 atmospheric models) and 18 (ATLAS9 and SYNTHE routines, spectral line data base). Cambridge, MA
Mackay D. H., Jardine M., Cameron A. C., Donati J.-F., Hussain G. A. J., 2004, MNRAS, 354, 737
Marsden S. C., Waite I. A., Carter B. D., Donati J.-F., 2005, MNRAS, 359, 711
Marsden S. C., Donati J.-F., Semel M., Petit P., Carter B. D., 2006, MNRAS, 370, 468
Marsden S. C., Berdyugina S. V., Donati J.-F., Eaton J. A., Williamson M. H., 2007, Astron. Nachr., 328, 1047
Morin J. et al., 2008, MNRAS, 390, 567
Petit P., Donati J.-F., Collier Cameron A., 2002, MNRAS, 334, 374
Reiners A., 2006, A&A, 446, 267
Savanov I. S., Strassmeier K. G., 2008, Astron. Nachr., 329, 364
Schrijver C. J., Title A. M., 2001, ApJ, 551, 1099
Schüssler M., Solanki S. K., 1992, A&A, 264, L13
Schüssler M., Caligari P., Ferriz-Mas A., Solanki S. K., Stix M., 1996, A&A, 314, 503
Siess L., Dufour E., Forestini M., 2000, A&A, 358, 593
Spruit H. C., 2002, A&A, 381, 923
Strassmeier K. G., Pichler T., Weber M., Granzer T., 2003, A&A, 411, 595

This paper has been typeset from a TEX/LATEX file prepared by the author.